

- Supplementary Data -

**Achieving fast interfacial solar vapor
generation and aqueous acid purification in
 $\text{Ti}_3\text{C}_2\text{T}_x$ MXene/PANI non-woven fabric**

Renjie Ding^a, Jinhua Xiong^a, Qian Yan^a, Zhong Chen^a, Zonglin Liu^a, Xu Zhao^a, Qingyu Peng^{a*}, and Xiaodong He^{a*}

^aNational Key Laboratory of Science and Technology on Advanced Composites in Special Environments, Center for Composite Materials and Structures, Harbin Institute of Technology, Harbin 150080, P. R. China

*Corresponding authors.



Figure S1. Digital image of $\text{Ti}_3\text{C}_2\text{T}_x$ dispersed in NMP (left) and $\text{Ti}_3\text{C}_2\text{T}_x$ DMAc dispersion at room temperature for 3 months (right).

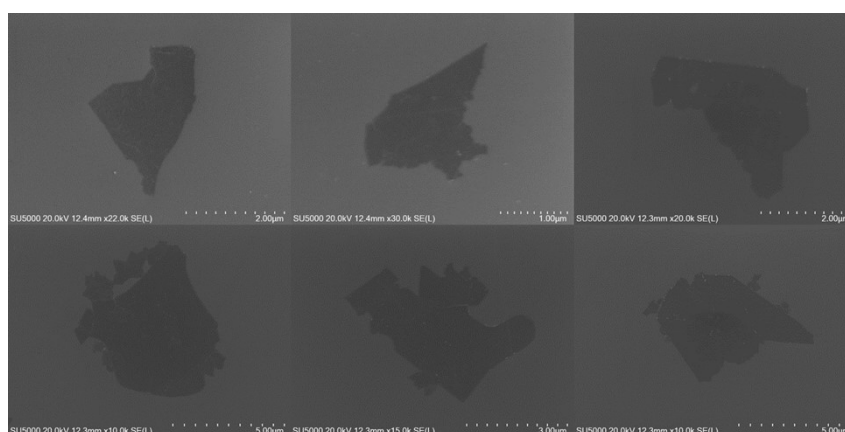


Figure S2. SEM image of $\text{Ti}_3\text{C}_2\text{T}_x$ nanosheets.

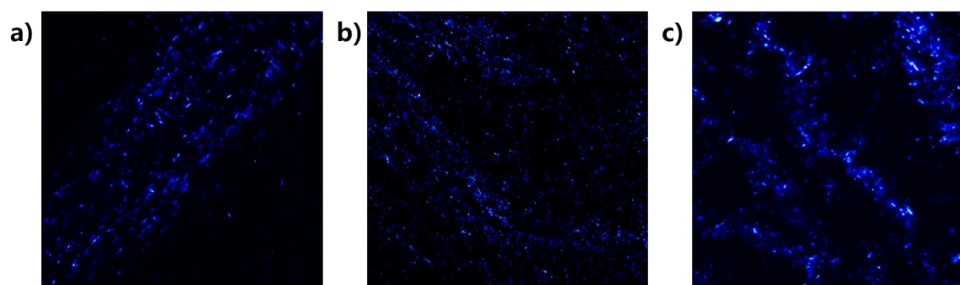


Figure S3. Liquid crystal of $\text{Ti}_3\text{C}_2\text{T}_x$ organic solvent dispersion. a) 15 mg/ml. b) 30 mg/ml. c) 40 mg/ml.

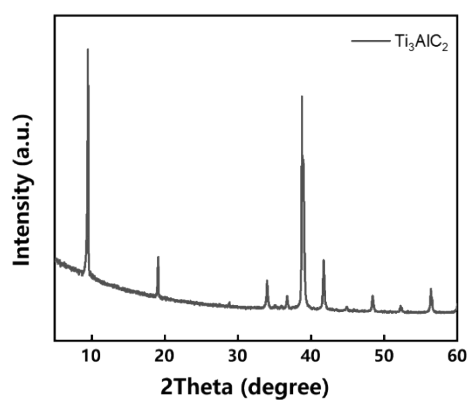


Figure S4. XRD pattern of MAX phase.

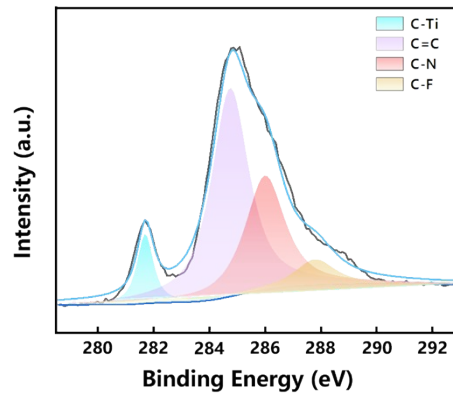


Figure S5. C 1S spectrum of MP1

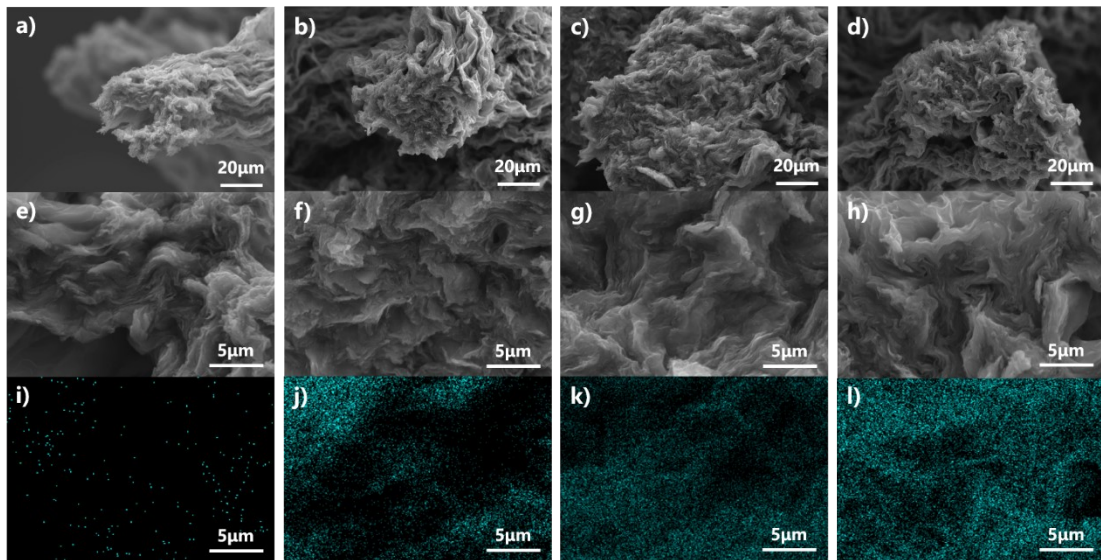


Figure S6. Cross sections and N mapping of composite fibers in MPs. a,e,i) MP0. b,f,j) MP1. c,g,k) MP2. d,h,l) MP3.

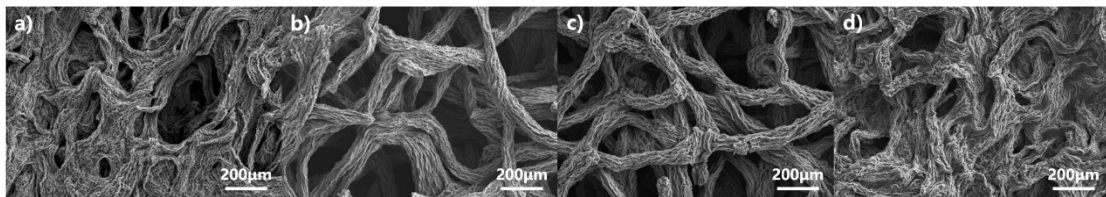


Figure S7. SEM image of MPs. a) MP0. b) MP1. c) MP2. d) MP3.

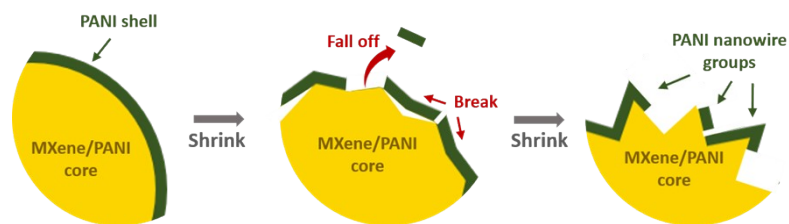


Figure S8. Schematic illustration of part of PANI falling off from composite fibers.

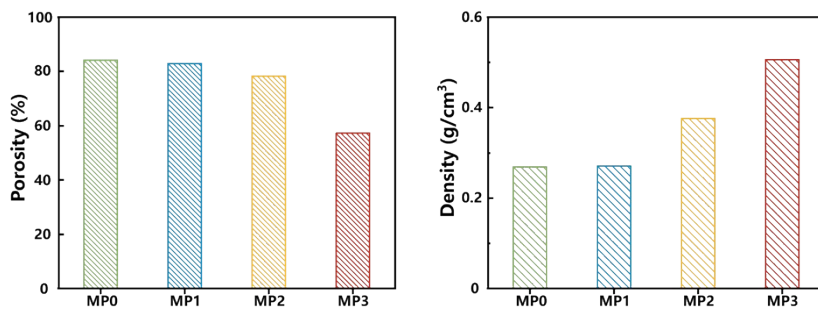


Figure S9. a) Porosity of MPs. b) Density of MPs.

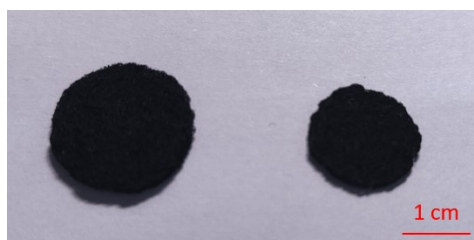


Figure S10. Digital image of MP1 (left) and MP3 (right).

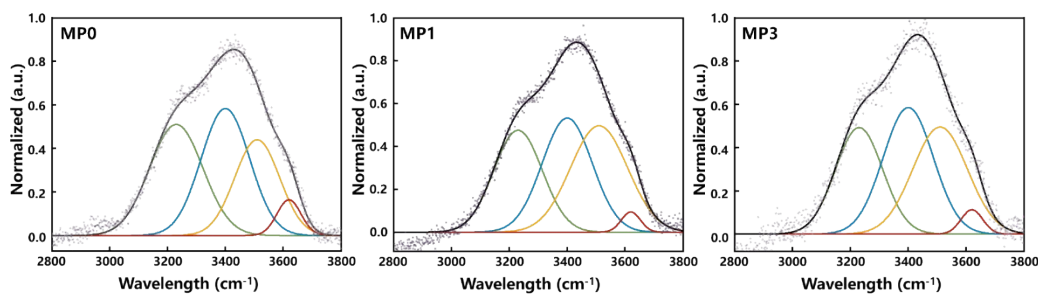


Figure S11. Raman spectra with fitting curves of MP0, MP1 and MP3.

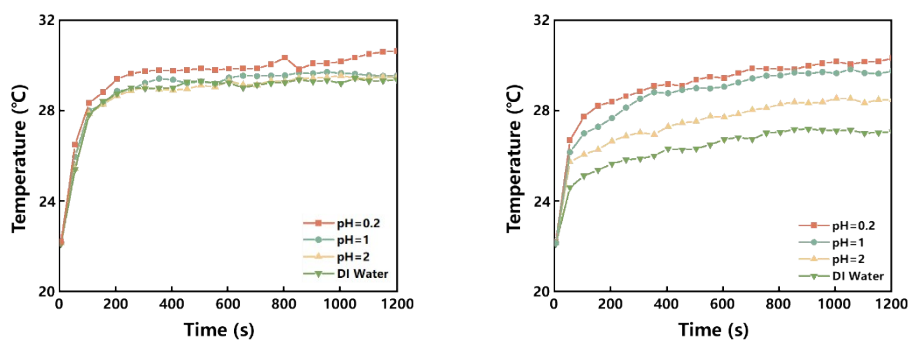


Figure S12. The surface temperature of MP1 (left) and MP2 (right) in water and aqueous acid with different pH value under one-sun illumination.

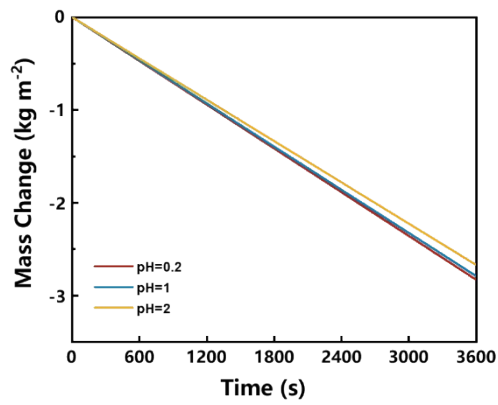


Figure S13. Time-dependent mass change of aqueous acid with MP2 working as steam generator.

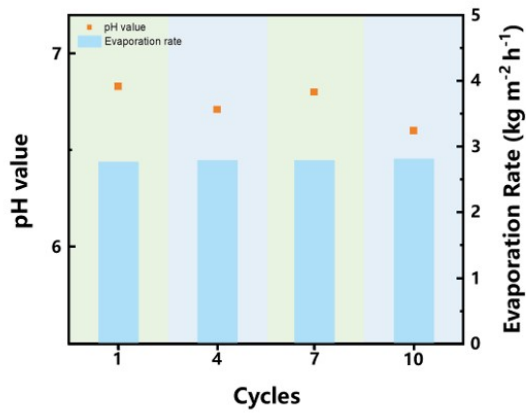


Figure S14. Cyclic tests of MP2 working as aqueous acid purifier and interfacial solar vapor generator in pH=1 aqueous acid.

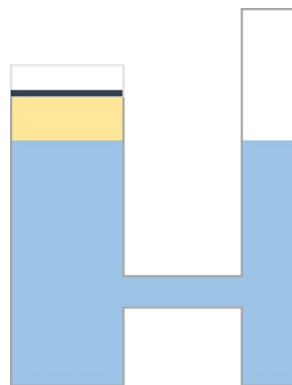


Figure S15. The designed water evaporation system for durable test.

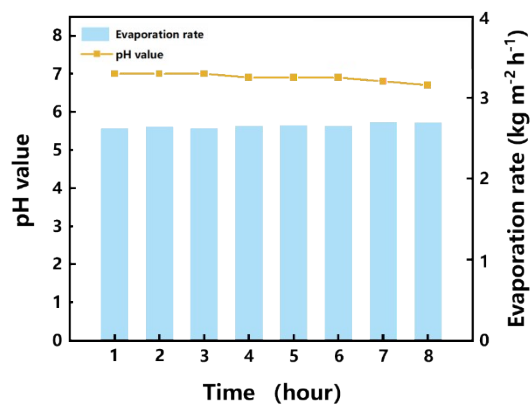


Figure S16. The durable test of MP2 in pH=4.5 aqueous acid.

Table S1. Comparison of solar vapor performances of MPs with other works.

Materials	Types	Light density (kW m ⁻²)	Evaporation rate (kg m ⁻² h ⁻¹)	Evaporation efficiency (%)	References
PANI/PA	Membrane	1	1.00		1
PANI/ZIF/PES	Membrane	1	1.07	66.8	2
PANI/PVDF	Membrane	1	1.09	74.15	3
PANI/TiO ₂ /Melamine	Bilayer aerogel	1	2.12	88.9	4
p-PEGDA/PANI	Hydrogel	1	1.4	91.5	5
Ti ₃ C ₂ T _x /PVA	Hydrogel	1	1.82	73.5	6
Ti ₃ C ₂ T _x /Porphyrin	Membrane	1	1.41	86.4	7
PANI/Graphene	Topographic PANI arrays	1	1.42	96.6	8
GO/PANI/ Ti ₃ C ₂ T _x	Flower-shaped aerogel	1	3.94	135.6	9
PDA/PEI/ Ti ₃ C ₂ T _x	Vertical yarns arrays	1	3.95	177.8	10
PANI/ Ti ₃ C ₂ T _x	Non-woven fabrics	1	2.65	93.7	This work

References

1. Wei, X., Peng, Y.B., Fang, W.X., Hu, Z.Y., Li, W.W., Zhang, S.X., and Jin, J. (2022). A polyaniline nanofiber array supported ultrathin polyamide membrane for solar-driven volatile organic compound removal. *Journal of Materials Chemistry A* *10*, 20424-20430. 10.1039/d2ta04909k.
2. Peng, Y.B., Wei, X., Wang, Y.J., Li, W.W., Zhang, S.X., and Jin, J. (2022). Metal-Organic Framework Composite Photothermal Membrane for Removal of High-Concentration Volatile Organic Compounds from Water via Molecular Sieving. *Acs Nano* *16*, 8329-8337. 10.1021/acsnano.2c02520.
3. Peng, Y.B., Wang, Y.J., Li, W.W., and Jin, J. (2021). Bio-inspired vertically aligned polyaniline nanofiber layers enabling extremely high-efficiency solar membrane distillation for water purification. *Journal of Materials Chemistry A* *9*, 10678-10684. 10.1039/d1ta01336j.
4. Pan, J.F., Yu, X.H., Dong, J.J., Zhao, L., Liu, L.L., Liu, J.L., Zhao, X.T., and Liu, L.F. (2021). Diatom-Inspired TiO₂-PANi-Decorated Bilayer Photothermal Foam for Solar-Driven Clean Water Generation. *Acs Applied Materials & Interfaces* *13*, 58124-58133. 10.1021/acsnano.1c16603.
5. Yin, X.Y., Zhang, Y., Guo, Q.Q., Cai, X.B., Xiao, J.F., Ding, Z.F., and Yang, J. (2018). Macroporous Double-Network Hydrogel for High-Efficiency Solar Steam Generation Under 1 sun Illumination. *Acs Applied Materials & Interfaces* *10*, 10998-11007. 10.1021/acsnano.8b01629.
6. Zhang, B., Wong, P.W., and An, A.K. (2022). Photothermally enabled MXene hydrogel membrane with integrated solar-driven evaporation and photodegradation for efficient water purification. *Chemical Engineering Journal* *430*, 133054. 10.1016/j.cej.2021.133054.
7. Zhang, B., Gu, Q., Wang, C., Gao, Q., Guo, J., Wong, P.W., Liu, C.T., and An, A.K. (2021). Self-Assembled Hydrophobic/Hydrophilic Porphyrin-Ti₃C₂T_x MXene Janus Membrane for Dual-Functional Enabled Photothermal Desalination. *Acs Applied Materials & Interfaces* *13*, 3762-3770. 10.1021/acsnano.1c16054.
8. Zhao, X., Meng, X., Zou, H., Wang, Z., Du, Y., Shao, Y., Qi, J., and Qiu, J. (2022). Topographic Manipulation of Graphene Oxide by Polyaniline Nanocone Arrays Enables High-Performance Solar-Driven Water Evaporation. *Advanced Functional Materials* *n/a*, 2209207. <https://doi.org/10.1002/adfm.202209207>.
9. Li, X.P., Li, X.F., Li, H.G., Zhao, Y., Wu, J., Yan, S.K., and Yu, Z.Z. (2022). Reshapable MXene/Graphene Oxide/Polyaniline Plastic Hybrids with Patternable Surfaces for Highly Efficient Solar-Driven Water Purification. *Advanced Functional Materials* *32*, 2110636. 10.1002/adfm.202110636.
10. Lei, Z., Zhu, S., Sun, X., Yu, S., Liu, X., Liang, K., Zhang, X., Qu, L., Wang, L., and Zhang, X. (2022). A Multiscale Porous 3D-Fabric Evaporator with Vertically Aligned Yarns Enables Ultra-Efficient and Continuous Water Desalination. *Advanced Functional Materials* *32*, 2205790. 10.1002/adfm.202205790.